

# Elucidation of the Corrosion Inhibition of Mild Steel in 1.0 M HCl by Catechin Monomers from Commercial Green Tea Extracts

S. NOFRIZAL, AFIDAH A. RAHIM, BAHRUDDIN SAAD, P. BOTHI RAJA, AFFAIZZA M. SHAH, and S. YAHYA

The inhibitive action of commercial green tea extracts on mild steel (MS) in a 1.0 M hydrochloric acid solution was investigated by weight loss, potentiodynamic polarization, and electrochemical impedance spectroscopy (EIS). A high-performance liquid chromatographic (HPLC) analysis showed conclusively that of the eight catechin monomers and caffeine found in the original extracts, only four components were responsible for the inhibition of MS. The decreasing adsorption capacity of monomers on MS is related to the stereochemistry of molecules and the number of phenolic groups, and it is as follows: epigallocatechin gallate > epicatechin gallate > epigallocatechin > epicatechin. Adsorption of green tea extract constituent was found to follow Langmuir adsorption isotherm and the calculated Gibb's free energy values indicated the physisorption of inhibitor over MS surface. Physisorption was supported well by the potential zero charge (PZC) and molecular surface energy-level calculations.

DOI: 10.1007/s11661-011-1030-3

© The Minerals, Metals & Materials Society and ASM International 2011

## I. INTRODUCTION

TEA is one of the most frequently consumed beverages in the world, dating back to more than 5000 years ago. Numerous studies have recorded the beneficial effects of tea, *e.g.*, reducing the risk of cancer,<sup>[1]</sup> preventing arteriosclerosis,<sup>[2]</sup> acting as an antiallergic agent,<sup>[3]</sup> providing antimicrobial properties,<sup>[4]</sup> and lowering the risk of stomach cancer<sup>[5]</sup> and lung cancer.<sup>[6]</sup> Previous studies have shown that green tea consists predominantly of flavan monomers, namely (+)-catechin, (+)-epicatechin, and alkaloids.<sup>[7]</sup> Interestingly, catechin also exhibits anti-oxidative activity which could reduce oxidation, corrosion, deterioration and discoloration processes.<sup>[8]</sup>

Corrosion is a common phenomenon in industries, and it attracts considerable amount of interest because of its hazardous nature on metals.<sup>[9]</sup> In many industries, acid solutions are used frequently for acid pickling, industrial cleaning, acid descaling, oil-well acid in oil recovery, and the petrochemical processes,<sup>[10–12]</sup> which leads to corrosive attack of metals. Generally, the inhibitors are used in these processes to control the metal dissolution as well as the acid consumption. Most of the inhibitors are organic molecules<sup>[13]</sup>; however, inorganic molecules<sup>[14]</sup> and polymeric materials<sup>[15]</sup> are also used. Although high anticorrosion potential was exhibited by many organic molecules, they pollute the environment during their synthesis and applications.<sup>[16]</sup>

Natural products are being studied for their corrosion-inhibition potential as they are more environmentally friendly, showing good inhibition efficiency with low risk of environmental pollution.<sup>[17,18]</sup> The use of natural compounds from plant extracts rich in tannins<sup>[19–21]</sup> *Rauvolfia serpentine*,<sup>[22]</sup> black pepper extract,<sup>[23]</sup> *Lawsonia*,<sup>[24]</sup> and *Opuntia* extract<sup>[25]</sup> have been reported widely by several authors.

The anticorrosion potential of tea waste,<sup>[26]</sup> as well as its constituent caffeine,<sup>[27,28]</sup> was reported previously. These studies concluded that the heterocyclic atoms of the caffeine molecule are responsible for its anticorrosion potential. The current study was inspired by the reports that green teas are characterized by the presence of catechin monomers that have been studied individually, which coincidentally are effective corrosion inhibitors.<sup>[8,29]</sup> Thus, this work aims at investigating the anticorrosion potential of a natural product *viz.*, catechin monomers derived from green tea extracts on mild steel (MS) in 1 M HCl medium. The assessment of the corrosion behavior has been studied using weight loss, electrochemical impedance spectroscopy (EIS), and potentiodynamic polarization measurements. High-performance liquid chromatography (HPLC) has been used for the first time to identify and quantify the active components of the green tea extracts simultaneously that are consumed during the corrosion-inhibition process.

## II. EXPERIMENTAL

### A. Inhibitor Preparation

Two green tea (GT) samples (*Camellia sinensis*) were purchased from a local supermarket and were produced from Cameron Highlands (GT 1), Malaysia, whereas the

S. NOFRIZAL and S. YAHYA, Master Students, AFIDAH A. RAHIM, Associate Professor, BAHRUDDIN SAAD, Professor, P. BOTHI RAJA, Postdoctorate Researcher, and AFFAIZZA M. SHAH, Ph.D. Student, are with the School of Chemical Sciences, Universiti Sains Malaysia, 11800 USM, P. Pinang, Malaysia. Contact e-mail: afidah@usm.my

Manuscript submitted August 11, 2011.

Article published online December 21, 2011

other one was of UK origin (GT 2). The green tea samples (10 g) were extracted in 100 mL water:acetonitrile:methanol (83:6:11) for 24 hours at 353 K (80 °C) by using the hot plate method.<sup>[30]</sup> The extract was cooled and centrifuged at 4000 rpm for 5 minutes. The sample was evaporated, and the resulting gummy material obtained was dried and grinded. Various concentrations of the tea extracts were prepared by dissolving known quantities of the resultant powder in 1 M HCl.

### B. Specimen Preparation

The MS specimens of composition (Fe: 97.57, C: 1.54, O: 0.88 wt pct) were taken and were polished using different grades of abrasive papers from 400 up to 1200 before the analysis. The MS specimens of size (2.7 × 2.7 × 0.1 cm) were used for the weight-loss studies, whereas specimens with an exposed area of 3.142 cm<sup>2</sup> were used for the electrochemical studies.

### C. Weight-Loss Method

The experiment was carried out in a beaker containing 50 mL test solution. A clean preweighed MS specimen was immersed completely in 50 mL electrolyte with and without the addition of different concentrations of GT extract at room temperature (303 K [30 °C ± 2]). After 24 hours of immersion in 1 M HCl solution, the specimen was withdrawn, rinsed with distilled water, washed with acetone, dried, and weighed. Triplicate measurements were performed. The inhibition efficiency (pct IE) was calculated as follows:

$$\text{pct IE} = \left(1 - \frac{W_i}{W_0}\right) \times 100 \quad [1]$$

where  $W_0$  and  $W_i$  are the weight loss of MS without and with inhibitor, respectively.

### D. Electrochemical Method

Electrochemical studies were carried out using Gamry Instrument reference 600 (potentiostat/galvanostat/ZRA) (Gamry Instruments, Warminster, PA). A three-electrode cell system was employed for the measurement; MS with an exposed area of 3.142 cm<sup>2</sup> acts as a working electrode (WE), whereas platinum wire and saturated calomel electrode acts as a counterelectrode and reference electrode (SCE), respectively. The measurements were performed in 1.0 M HCl solution with and without the addition of different inhibitor concentrations in an aerated environment. All polarization and impedance curves were recorded at room temperature 303 K (30 ± 2 °C), and the electrodes were immersed in the test solution for 30 minutes at natural potential to attain steady state before measurement. Electrochemical impedance spectroscopy was carried out at the corrosion potential ( $E_{\text{corr}}$ ) with frequency ranging from 0.1 to 10000 Hz at an amplitude of 10 mV. The impedance diagrams are given in the Nyquist representation. Inhibition efficiency is calculated from the charge-transfer resistance ( $R_{\text{ct}}$ ) values by using Eq. [2].

$$\text{pct IE} = \left(1 - \frac{R_{\text{ct}(0)}}{R_{\text{ct}(i)}}\right) \times 100 \quad [2]$$

where  $R_{\text{ct}(0)}$  and  $R_{\text{ct}(i)}$  is the charge-transfer resistance of MS without and with inhibitor, respectively.

The potentiodynamic current density—potential curves were recorded by scanning the electrode potential from −800 to −200 mV (*vs* SCE) with a scanning rate of 1 mV seconds<sup>−1</sup>. The linear Tafel segments of the anodic and cathodic curves were extrapolated to corrosion potential to obtain the corrosion current densities ( $i_{\text{corr}}$ ). Equation [3] shows the calculation of pct IE from the  $i_{\text{corr}}$  values.

$$\text{pct IE} = \left(1 - \frac{i_{\text{corr}(i)}}{i_{\text{corr}(0)}}\right) \times 100 \quad [3]$$

where,  $i_{\text{corr}(i)}$  and  $i_{\text{corr}(0)}$  is the corrosion current density of MS with and without inhibitor, respectively.

### E. Determination of Potential Zero Charge (PZC)

The PZC of MS in the absence and presence of all concentrations of green tea extract was determined using Gamry Instrument reference 600 (potentiostat/galvanostat/ZRA). The maximum frequencies ( $F_{\text{max}}$ ) of all samples with inhibitor and without inhibitor were identified from the Bode plot in the EIS studies. The initial and final potential range was set at −1 to 0.5 V at each  $F_{\text{max}}$ .

### F. Fourier Transformed Infrared (FTIR) Spectroscopic Analysis

The green tea extracts were analyzed by FTIR spectroscopy for the identification of the functional groups. The FTIR study was carried out by using the PerkinElmer System 2000 FT IR instrument (PerkinElmer, Inc., Waltham, MA) in the IR range of 400 to 4000 cm<sup>−1</sup>. The pellet for the solid sample was prepared by using the KBr pellet method with the ratio of the sample to KBr was 1:10. The mixture was then pressed with 8-ton pressure to obtain a pellet. The acquisition of the spectra and peaks assignment was performed using FTIR software Spectrum Version 3.02.01 (PerkinElmer, Inc., Waltham, MA).

### G. HPLC Analysis

The HPLC system used consisted of two LC-10 AD VP pumps for high-pressure gradient elution attached with a SPD-10Avp UV detector (Shimadzu, Kyoto, Japan). The mobile phase composition comprises water:acetonitrile:methanol (83:6:11). The column used was a monolithic Rp-18 e 100–4.6 mm (Merck KGaA, Straße, Germany). The signals were monitored at 280 nm. Standard solutions and tea samples were filtered through a 0.45-μm acrylic polymer filter before being injected into the HPLC unit. Quantification was done using the external calibration method where peaks areas *vs* concentrations were plotted. A linear least-square analysis on the straight line was used for the

quantification, whereas a qualitative analysis was based on a comparison of the retention times of standards. Twenty microliters of the analytical samples were injected. The concentrations of the catechin monomers in corrosive media were also determined by means of HPLC technique. For this, a standard dose (5 mL) of corrosive media before and after the prescribed corrosion studies (weight loss and polarization) was taken for the HPLC analysis, in which the pH has been adjusted to 2.5 by using 5 M sodium hydroxide solution. From this sample, a small quantity (1 mL) was filtered off by using syringe filters (13 mm 0.45  $\mu\text{M}$ ), and 20  $\mu\text{L}$  was injected into the HPLC unit for the analysis.

#### H. Molecular Modeling Studies

The energy levels *viz.*, highest occupied molecular orbital (HOMO) and lowest unoccupied molecular orbital (LUMO) for various catechin monomers were calculated using the Restricted Hartree-Fock level PM3 method in MOPAC 2000 program of CS ChemOffice 8.0 version (License number: 7654321).

### III. RESULTS AND DISCUSSION

#### A. Weight Loss Measurement

The pct IE obtained for different concentrations of green tea extract is depicted in Table I. The results show a positive correlation between the concentration of green tea extract and the inhibition efficiency for MS in 1 M HCl solution. This trend may result from the fact that the amount adsorbed and the coverage of inhibitor molecules on the MS surface increased with the increase of the green tea extract concentration, thus the MS surface is blocked efficiently from the hydrochloric acid. The maximum pct IE was obtained at maximum concentration of 200 mg L<sup>-1</sup> for both green tea extracts and was found to be 81.54 and 84.73 for GT 1 and GT 2, respectively.

#### B. Potentiodynamic Polarization Measurements

Polarization results are depicted as Tafel plots in Figures 1(a) and (b). The various corrosion parameters *viz.*, corrosion potential  $E_{\text{corr}}$ , corrosion current density

$i_{\text{corr}}$ , cathodic ( $\beta_c$ ), anodic ( $\beta_a$ ), Tafel slopes, and (pct IE) were calculated using the intersection of the anodic and cathodic Tafel lines and are given in Table II.

It is clear from the potentiodynamic experimental results that the presence of tea extracts reduces the corrosion current density  $i_{\text{corr}}$ , which is an indication of the decrease in the corrosion rate. The decrease in  $i_{\text{corr}}$  values is caused by the decrease of the aggressive acid attack on the MS surface, which is attributed to the adsorption of inhibitor molecule. Furthermore, the additions of tea extract shift the corrosion potential to the positive side (35 mV for GT 1 and 43 mV for GT 2) because of the decrease in the anodic reaction. This indicated that the inhibitors were adsorbed on the anodic sites of the MS surface, which prevented the metal dissolution reaction and thus controlled the corrosion process. However, significant changes in Tafel constant values  $\beta_c$  and  $\beta_a$  were observed with the addition of inhibitors from that of the blank, indicating that the inhibitor prevents the metal corrosion by controlling both hydrogen evolution reaction at the cathodic site and metal dissolution at the anodic site. The pct IE was found to enhance when the concentration of the green tea extract was increased, resulting in maximum of 85.80 for GT 1 and 90.01 for GT 2 extracts, respectively. The results obtained are in good agreement with those obtained from the weight-loss measurements.

**Table I. Effect of Green Tea Extracts for the Corrosion of MS in 1.0 M HCl (Weight-Loss Studies)**

Inhibitor	Concentration (ppm)	Weight Loss (g)	Pct IE (wt pct)
—	0	0.0439	—
GT 1	50	0.0251	42.84
	100	0.0173	60.59
	150	0.0125	71.52
	200	0.0081	81.54
GT 2	50	0.0222	49.43
	100	0.0135	69.25
	150	0.0089	79.74
	200	0.0067	84.73

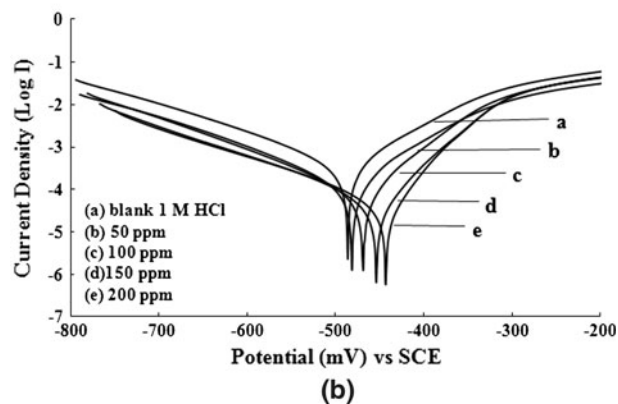
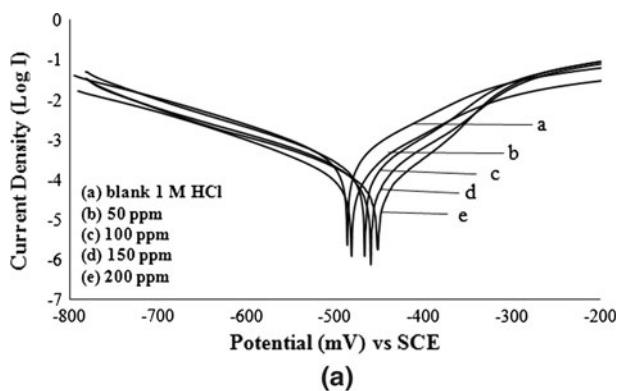


Fig. 1—Tafel plots of (a) GT 1 and (b) GT 2 extracts on MS in 1 M HCl.

**Table II. Effect of Green Tea Extracts for the Corrosion of MS in 1.0 M HCl (Polarization Studies)**

Inhibitor	Concentration (ppm)	$E_{\text{corr}}$ (mV)	$i_{\text{corr}}$ ( $\mu\text{A cm}^{-2}$ )	$\beta_a$ ( $\text{mV dec}^{-1}$ )	$-\beta_c$ ( $\text{mV dec}^{-1}$ )	Pct IE
—	0	-486	388.1	88.3	147.2	—
GT 1	50	-479	132.9	87.2	152.3	65.82
	100	-466	93.2	40.8	94.7	75.91
	150	-460	71.6	32.3	81.1	81.53
	200	-451	54.9	30.2	75.6	85.80
GT 2	50	-481	120.9	86.2	155.3	68.82
	100	-469	83.4	85.4	143.2	78.51
	150	-454	50.1	78.5	132.5	87.13
	200	-443	38.8	42.7	114.4	90.01

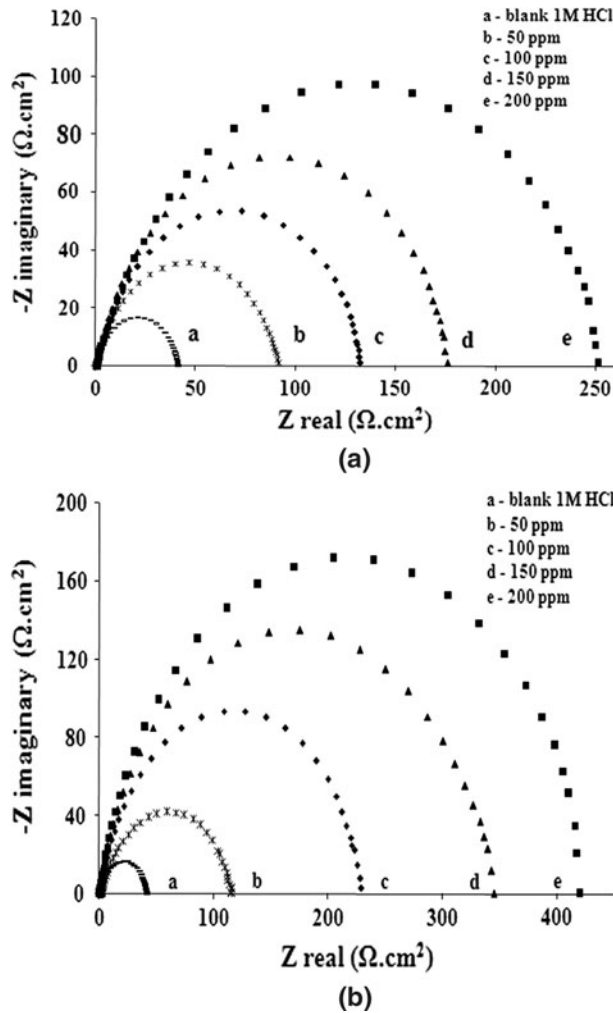


Fig. 2—Nyquist plots of (a) GT 1 and (b) GT 2 extracts on MS in 1 M HCl.

**C. EIS**

EIS analysis shows typical Nyquist plots and Bode plots for GT 1 and GT 2 extracts, which are given in Figures 2 and 3(a) and (b), respectively. One constant phase element (CPE) was substituted for the capacitive element ( $C_{dl}$ ) with double-layer capacitance to give a more accurate fit,<sup>[31]</sup> as the obtained capacitive loop is a depressed semicircle rather than a regular one. The

impedance parameters, *viz.*, charge-transfer resistance ( $R_{ct}$ ) and CPE were calculated by analyzing the impedance plots using the equivalent circuit (Figure 4), and the values are listed in Table III. The usefulness of these data permits the analysis of the electrochemical impedance data, which are based on the modeling of a corrosion process by an electrical circuit.<sup>[32]</sup> From Figures 2(a) and (b), it was observed that the Nyquist plots showed slightly depressed semicircular shapes with only one time constant, and the diameters of the capacitive loop increased with increasing inhibitor concentration. This indicates the increasing coverage of the metal surface and also signifies a charge-transfer process as the main controlling factor in the corrosion process.<sup>[33]</sup> The presence of one phase maximum was observed in Bode plots (Figures 3(a) and (b)) at intermediate frequencies, which indicated the presence of one time constant corresponding to the impedance of the formed protective film.<sup>[34]</sup>

Furthermore, it is also observed from Table III that the  $R_{ct}$  values increased with increasing concentrations of inhibitors. This is because the addition of inhibitor increases the adsorption of phytoconstituents over the MS surface and results in the formation of a protective layer, which may decrease the charge transfer between the metal surface and the corrosive medium. The values of CPE decrease with the increase in inhibitor concentrations as a result of the addition of inhibitor that increases the adsorption phenomena, which consequently may decrease the electrical capacity and/or increase in the thickness of the electrical double layer.<sup>[35]</sup> The pct IE of impedance results are in good agreement with the polarization and weight-loss studies that shows maximum of 83.21 and 90.13 for GT 1 and GT 2 extracts, respectively, for the maximum concentration of 200 mg L<sup>-1</sup>.

**D. Adsorption Isotherm**

To examine the adsorption behavior of the green tea extracts on the MS surface in 1 M HCl medium, the adsorption isotherm was plotted. The dependence of the fraction of the surface covered ( $\theta$ ) obtained by the ratio of  $IE/100$  as a function of the logarithm of the concentration ( $\log C$ ) of tea extracts was tested graphically by fitting it to several adsorption isotherms. The experimental data from all measurements was found to



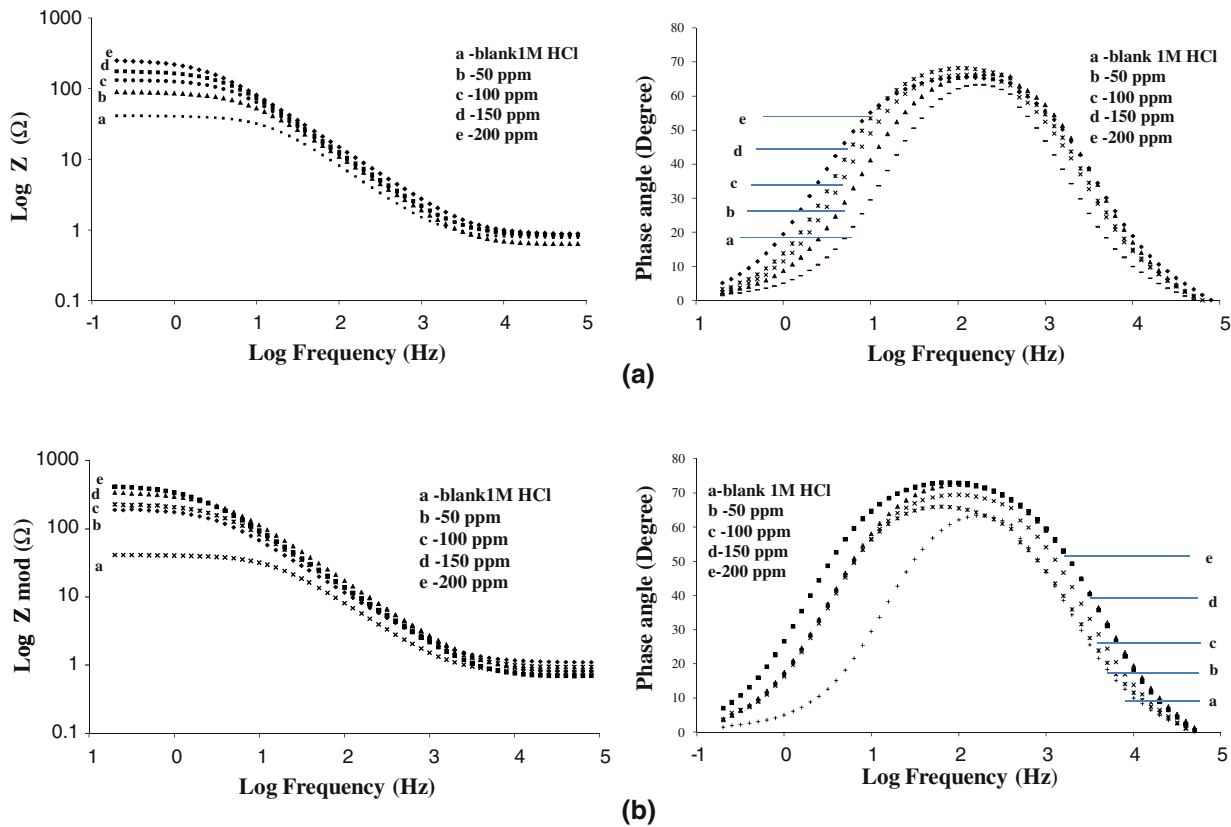


Fig. 3—Bode plots of (a) GT 1 and (b) GT 2 extracts on MS in 1 M HCl.

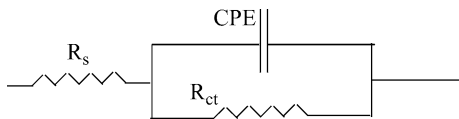


Fig. 4—Electrical equivalent circuit for electrochemical impedance measurement.

fit well with the Langmuir adsorption isotherm and are depicted in Figures 5(a) through (c) for weight-loss study, polarization, and impedance studies respectively, which obeys the following equation<sup>[36]</sup>:

$$\frac{C}{\theta} = \frac{1}{K_{\text{ads}}} + C \text{ and } \Delta G_{\text{ads}}^{\circ} = -RT \ln C_{\text{water}} K_{\text{ads}} \quad [4]$$

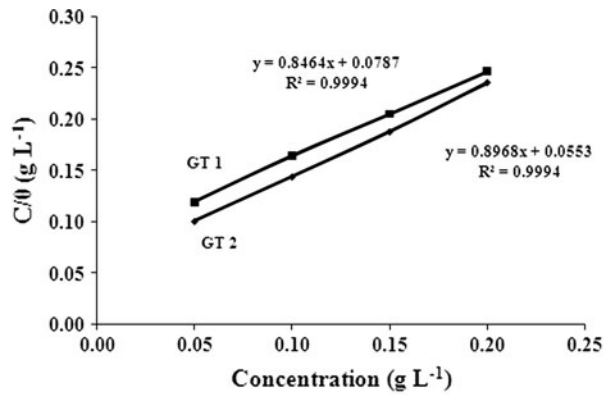
where  $C$  is the concentration of inhibitor,  $\theta$  is the surface coverage determined by  $\text{IE}/100$ ,  $K_{\text{ads}}$  is the adsorption equilibrium constant and  $\Delta G_{\text{ads}}^{\circ}$  is the standard Gibbs free energy,  $R$  is the molar gas constant,  $T$  is the temperature, and  $C_{\text{water}}$  is the concentration of water in  $1000 \text{ g L}^{-1}$ . The Gibbs free energy values ( $\Delta G_{\text{ads}}^{\circ}$ ), linear regression coefficient, and adsorption – desorption equilibrium constant ( $K_{\text{ads}}$ ) derived from the Langmuir plot are depicted in Table IV.

The negative values of  $\Delta G_{\text{ads}}^{\circ}$  revealed the spontaneity of the adsorption process. Generally,  $\Delta G_{\text{ads}}^{\circ}$  values at approximately  $-20 \text{ kJ mol}^{-1}$  or lower are associated

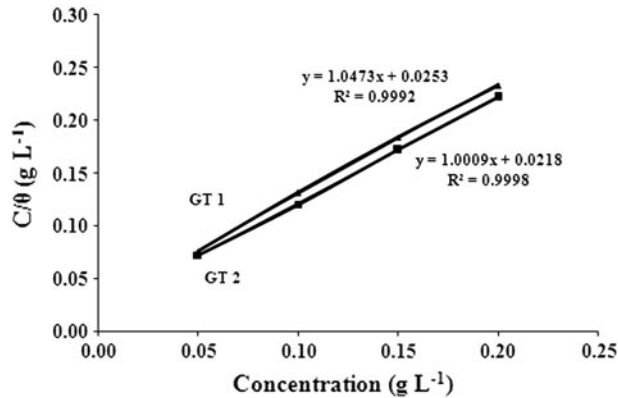
Table III. Effect of Green Tea Extracts for the Corrosion of MS in 1.0 M HCl (Impedance Studies)

Inhibitor	Concentration (ppm)	$R_{\text{ct}}$ ( $\Omega \text{ cm}^2$ )	CPE ( $\mu\text{F cm}^{-2}$ )	Pct IE
—	0	41.4	48.7	—
GT 1	50	91.9	29.1	54.37
	100	132.4	24.2	68.43
	150	175.9	21.4	76.54
	200	251.2	17.0	83.21
GT 2	50	115.8	34.9	63.55
	100	288.9	27.6	81.78
	150	344.9	22.7	87.93
	200	419.9	19.6	90.13

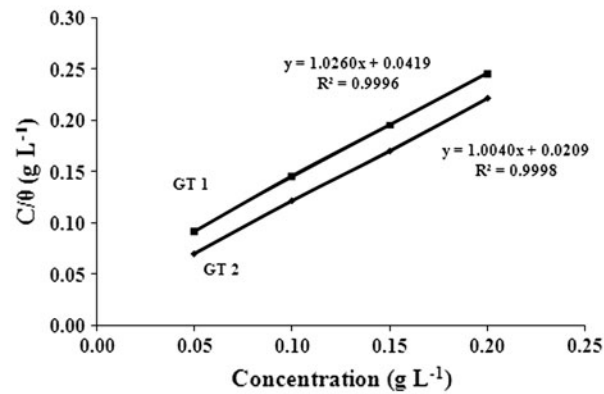
with electrostatic interactions between the charged centers of inhibitors and charged metal surface (physisorption). Values more negative than  $-40 \text{ kJ mol}^{-1}$  involve charge sharing or transfer from the inhibitor molecules to the metal surface to form a coordinate type of bond (chemisorption).<sup>[37,38]</sup> The calculated  $-\Delta G_{\text{ads}}^{\circ}$  values for all the studies are depicted in Table IV. The  $-\Delta G_{\text{ads}}^{\circ}$  values were found to range between  $-23$  and  $-27 \text{ kJ mol}^{-1}$  for both green tea extracts, which evidenced the typical physisorption of inhibitors on MS surface. The higher  $K_{\text{ads}}$  values obtained for GT 2 suggested that this inhibitor was adsor-



(a)



(b)



(c)

Fig. 5—Langmuir adsorption isotherm plots for (a) weight loss, (b) polarization, and (c) impedance methods.

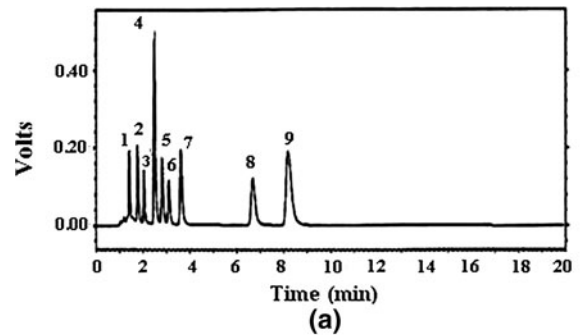
bed more strongly onto the MS surface compared with GT 1.<sup>[39]</sup>

### E. HPLC Analysis

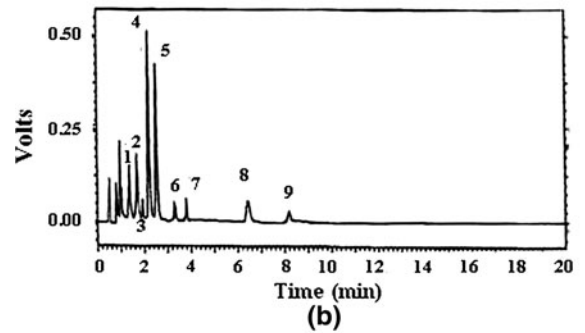
The concentrations of the catechin monomers and caffeine in the green tea extracts were determined using the HPLC technique. This method is by far the most popular technique for analyzing tea catechins. Wang *et al.*<sup>[40]</sup> reported on the use of methanol/water and acetonitrile/water as mobile phase for the catechin analysis. The catechin monomers and caffeine were

Table IV. Adsorption Isotherm Parameters

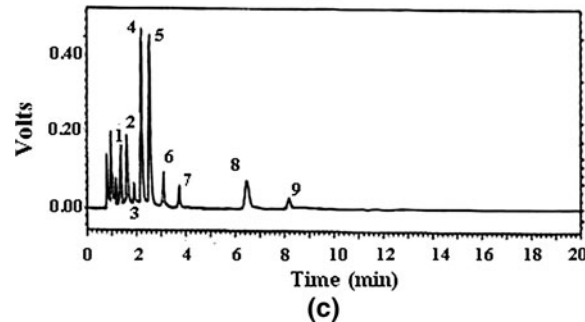
Inhibitor	Methods	$R^2$	$K_{ads}$ ( $L g^{-1}$ )	$\Delta G_{ads}^{\circ}$ ( $kJ mol^{-1}$ )
GT 1	Weight loss	0.9994	13.51	-23.96
	Potentiodynamic	0.9992	23.86	-25.39
	EIS	0.9996	25.45	-25.56
GT 2	Weight loss	0.9994	18.08	-24.69
	Potentiodynamic	0.9998	26.74	-25.67
	EIS	0.9998	35.97	-26.43



(a)



(b)



(c)

Fig. 6—HPLC chromatogram of (a) standard catechins and caffeine, (b) GT 1 and (c) GT 2 extracts. Peak assignment: (1) (-)-GC, (2) (-)-EGC, (3) (-)-C, (4) (-)-caffeine, (5) (-)-EGCG, (6) (-)-EC, (7) (-)-GCG, (8) (-)-ECG, and (9) (-)-CG.

separated in approximately 40 minutes. In contrast to all previous HPLC analyses that use the particle-type stationary phase, the current study uses a monolithic column. The use of highly porous monolithic columns has resulted in many advantages to the user (*e.g.*, minimum back pressures, faster separations, and consumption of less mobile phases). In the current

study, the optimized isocratic system comprising water:acetonitrile:methanol (83:6:11) as mobile phase was used and satisfactory separation of the catechins and caffeine was obtained using a flow rate of 1.4 mL minute<sup>-1</sup> (Figure 6). All components were separated in approximately 8 minutes. The separation was comparatively faster than the previous reports<sup>[40-42]</sup> that are based on conventional particle-type stationary phase. Nine peaks were observed for the tea extracts, and their concentrations are given in Table V. Based on the retention times, the peaks were identified as GC, EGC, C, caffeine, EGCG, EC, GCG, ECG, and CG. The order of elution was as follows: GC > EGC > C > caffeine > EGCG > EC > GCG > ECG > and > CG.

To determine the anticorrosion components of tea extracts, an HPLC analysis of test solutions was carried out before and after the corrosion processes. The concentrations of catechin consumed after the inhibition process from the potentiodynamic polarization measurement and weight-loss measurements are given in Table VI. In a previous study,<sup>[29]</sup> it was

**Table V. Determination of Catechins and Caffeine Green Tea Samples by HPLC Analysis**

Analytes	Concentration (mg g <sup>-1</sup> )	
	GT 1	GT 2
GC	4.21 ± 0.41	5.32 ± 0.91
EGC	17.04 ± 0.65	17.92 ± 0.15
C	2.34 ± 0.20	2.56 ± 0.49
Caffeine	35.74 ± 0.15	38.68 ± 0.84
EGCG	33.72 ± 0.15	36.08 ± 0.53
EC	8.32 ± 0.23	9.08 ± 0.23
GCG	2.65 ± 0.33	2.53 ± 0.16
ECG	9.48 ± 0.07	10.24 ± 0.06
CG	0.15 ± 0.02	0.28 ± 0.03

n = 3.

C, catechin; CG, catechin gallate; EC, epicatechin; ECG, epicatechin gallate; EGC, epigallocatechin; EGCG, epigallocatechin gallate; GC, gallic catechin; GCG, gallic catechin gallate.

assumed that all monomers act as inhibitors for steel corrosion and their inhibitive performance depended on their concentrations. However, a key finding of this study was that only certain catechin monomers gave significant contributions to the corrosion inhibition. Among the eight catechin monomers present in the tea extract, only EC, EGC, ECG, and EGCG were found to be consumed in the inhibition process as witnessed from the marked reduction of peak areas in the HPLC chromatogram. The peak areas for the other components were virtually unchanged. The order of increasing consumption and, thus, adsorption is as follows: EC < EGC < ECG < EGCG. Interestingly, none of the chiral counterparts [(C), (GC), (GCG), and (CG)] were found to participate in the inhibition process, although some of these monomers have shown inhibitive effects when used individually.<sup>[29]</sup> This suggests that the inhibition is stereospecific and the (R, R) conformation (Table VII) may have facilitated the adsorption of these molecules.

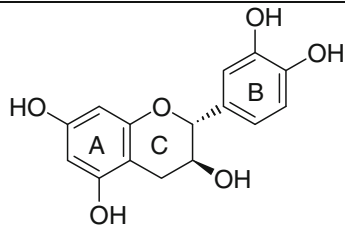
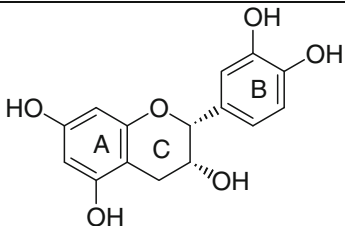
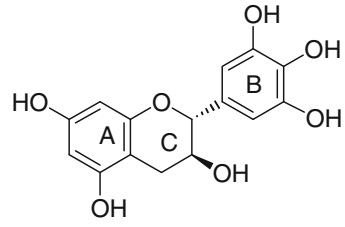
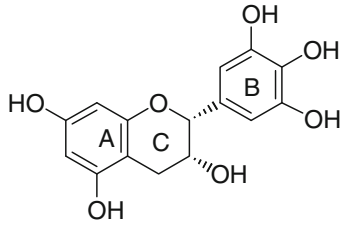
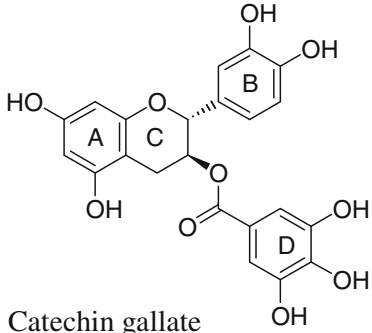
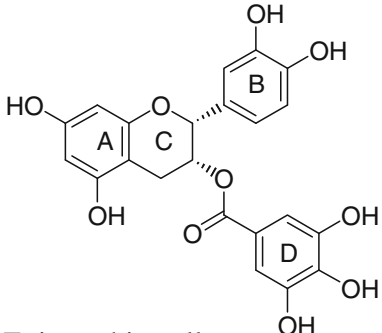
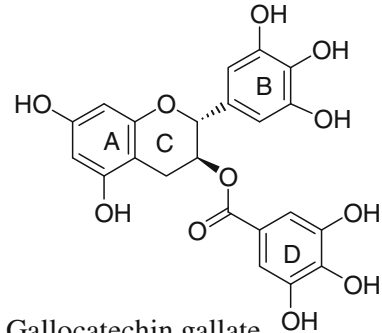
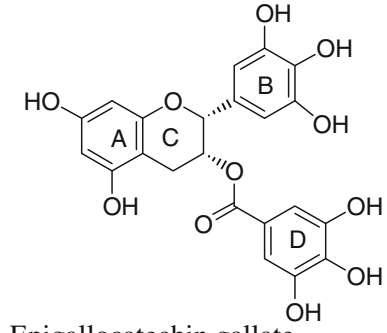
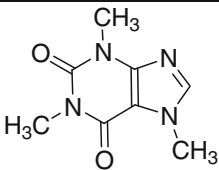
The higher overall content of GT 2 extract showed higher consumption of the monomers, which is consistent with the higher inhibition efficiency of the GT 2 extract compared with the GT 1 extract. The amount of monomers consumed also showed a positive correlation with the time of immersion where higher consumption of monomers was recorded for the weight-loss method. Surprisingly, although both tea extracts contain significant amount of caffeine, the HPLC results did not show the consumption of caffeine alkaloid. This contradicts with previous studies that reported caffeine as an effective metal corrosion inhibitor in various electrolytes.<sup>[27,28,43]</sup> This disparity could occur because the presence of the catechin monomers (EC, EGC, ECG, and EGCG) may have blocked the adsorption of caffeine molecule over the MS surface or because of the different electrolyte used. To confirm this, we conducted experiments on caffeine standards using our current system. Our results showed that the caffeine did not give any inhibition for all concentrations tested in 1 M HCl.

**Table VI. Consumption of Catechin Monomers after the Corrosion Process Determined by HPLC Analysis**

Inhibitor	Catechin Monomers	Amount Consumed			
		Polarization Study		Weight-Loss Study	
		mg g <sup>-1</sup>	Pct	mg g <sup>-1</sup>	Pct
GT 1	EC	0.18	2.16 ± 0.25	0.57	6.85 ± 0.41
	EGC	0.48	2.82 ± 0.13	1.66	8.51 ± 0.31
	ECG	0.38	4.01 ± 0.13	0.08	12.34 ± 0.33
	EGCG	1.89	5.60 ± 0.55	4.56	15.18 ± 0.16
GT 2	EC	0.25	2.75 ± 0.61	0.71	7.82 ± 0.39
	EGC	0.68	3.79 ± 0.32	2.01	11.16 ± 0.21
	ECG	0.54	5.27 ± 0.42	1.44	14.06 ± 0.18
	EGCG	2.21	6.12 ± 0.11	5.88	16.29 ± 0.23

n = 3.

Table VII. Structures of Catechin Monomers and Caffeine

R, S conformation	R, R conformation
 <p data-bbox="520 474 679 506">Catechin (C)</p>	 <p data-bbox="911 468 1126 499">Epicatechin (EC)</p>
 <p data-bbox="480 747 711 779">Gallocatechin (GC)</p>	 <p data-bbox="906 747 1198 779">Epigallocatechin (EGC)</p>
 <p data-bbox="453 1094 651 1157">Catechin gallate (CG)</p>	 <p data-bbox="863 1115 1102 1178">Epicatechin gallate (ECG)</p>
 <p data-bbox="448 1503 703 1566">Gallocatechin gallate (GCG)</p>	 <p data-bbox="863 1503 1150 1566">Epigallocatechin gallate (EGCG)</p>
 <p data-bbox="799 1770 906 1801">Caffeine</p>	



## F. FT IR Studies

The green tea extracts were studied by FTIR spectroscopy to identify the functional groups. Figure 7 shows the IR absorption spectrum of the green tea extracts and the typical functional groups of catechin namely O-H, C=C (for aromatic rings), and C-O that were evidenced at 3400 to 3100, 1600, and 1150 to 1010  $\text{cm}^{-1}$ , respectively.<sup>[44]</sup> These functional groups were identified already as potent anticorrosion groups in organic corrosion inhibitors as reported by many researchers.<sup>[45]</sup>

It was assumed that a catechin monomer that has more numbers of hetero functionality and  $\pi$ -electronic clouds could serve as a better corrosion inhibitor. According to this consideration, an EGCG monomer was assumed to contribute more during the corrosion inhibition process because it has three aromatic rings along with eight OH groups, whereas ECG contains seven OH groups and EC. EGC has fewer aromatic rings and OH groups. Indeed, as mentioned, the HPLC results showed that an EGCG monomer was consumed the most during the inhibition process, suggesting that the presence of heterofunctional groups (OH) and  $\pi$ -electrons on the benzene ring contributed to the corrosion inhibition by EGCG.

## G. Molecular Modeling Studies

Electrochemical techniques coupled with surface analytical techniques can provide basic information on the mechanism of corrosion inhibition. A need exists for a systematic approach for the characterization of the interaction between the organic inhibitor molecule and the metal or alloy. Theoretical approaches provide useful means of analyzing these interactions. Furthermore, the quantum level calculation of molecules can explain also the mechanism of corrosion inhibition.<sup>[46]</sup>

Table VIII shows the HOMO and LUMO surface images of catechin monomers *viz.*, EC, EGC, ECG, and EGCG.

The orbitals are represented by colored lobes (red/blue). Red represents more negative and blue represents less negative regions of electronegativity (electron density). The colored lobes also indicated the presence of  $\pi$  electron (electrons of  $\pi$  bonds) clouds over the phenyl rings. From the HOMO-LUMO images, it is obvious that the electron density was found to localize on either one of the aromatic rings and on hetero functional groups.

The HOMO-LUMO energy levels for various catechin monomers were calculated. The relevant quantum parameters are listed in Table IX.  $E_{\text{HOMO}}$  values are often associated with the electron-donating ability of the molecule, and the high  $E_{\text{HOMO}}$  values indicate that the molecule has a tendency to donate electrons to appropriate acceptor molecules with low-energy empty molecular orbital. Increasing values of the  $E_{\text{HOMO}}$  facilitate adsorption (and therefore inhibition) by influencing the transport process through the adsorbed layer.

The  $E_{\text{LUMO}}$  values represent the electron-acceptor ability of a molecule; lower values increases the electron-accepting capacity. In addition, the energy gap ( $\Delta E$ ) implies high stability for the molecule in chemical reactions<sup>[47]</sup>; higher values prevent the interelectron transfer that may prefer the electron donation to MS.<sup>[17]</sup> From Table IX, it is found that the  $\Delta E$  values obtained are similar to each other and follow the order  $\text{EGC} > \text{EC} > \text{ECGC} > \text{ECG}$ , which are not consistent with the HPLC results. This observation implies that the inhibition process did not proceed through electron transfer or acceptance in the interaction between the inhibitor molecule and MS surface.<sup>[48]</sup> So, the green inhibitors probably are adsorbed physically over the MS surface, and the interactions between the inhibitor and

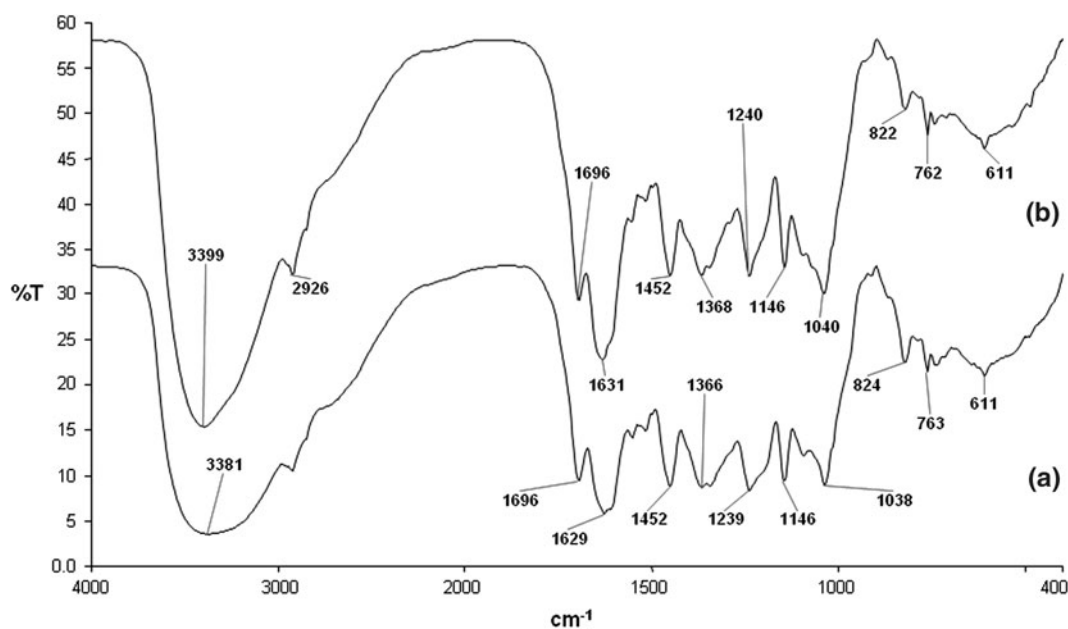


Fig. 7—IR spectra of (a) GT 1 and (b) GT 2 extracts.

Table VIII. The Electron Density Distribution of Catechin Monomers (EC, EGC, ECG and EGCG)

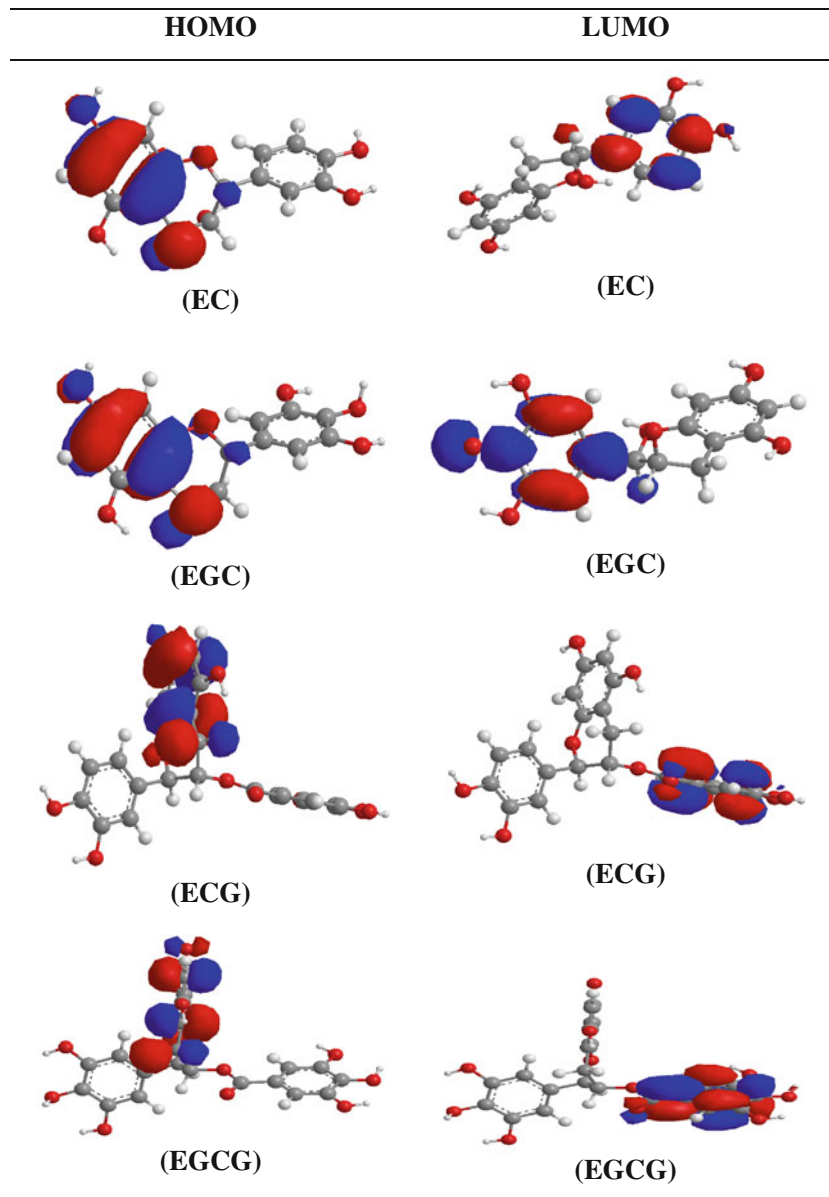


Table IX. Quantum Parameters for Catechin Monomers

Energy Levels	EC	EGC	ECG	EGCG
$E_{HOMO}$ (eV)	-8.938	-8.941	-9.011	-9.053
$E_{LUMO}$ (eV)	-0.196	-0.185	-0.533	-0.497
$\Delta E$ ( $E_{HOMO-LUMO}$ )(eV)	-8.742	-8.756	-8.478	-8.556

MS surface is probably ascribed to  $\pi$ - $\pi$  orbital interaction.

#### H. PZC and the Inhibition Mechanism

The PZC is useful in determining the type of adsorption of inhibitors that occurs at the electrode surface.<sup>[49]</sup> The surface charge of the metal is defined by the position of the open-circuit potential with respect to

the PZC,<sup>[50]</sup> and it was found by using the equation  $E_r = E_{ocp} - E_{PZC}$ , where  $E_r$  is Antropov's "rational" corrosion potential.<sup>[51]</sup> The calculated PZC values are presented in Table X.

When the difference  $E_r$  value is negative, cationic adsorption is favored, whereas positive difference results in anionic adsorption.<sup>[50,51]</sup> The results showed positive values of  $E_r$ , which indicated that the positively charged MS surface may be adsorbed specifically by the chloride ions (anions). Furthermore, the protonated inhibitor molecule may adsorb on the MS surface via chloride ions forming interconnecting bridges between the positively charged MS surface and the protonated inhibitors.<sup>[51]</sup> However, the adsorption may not be in direct physical contact with the metal and can be desorbed easily. This finding is consistent with the thermodynamic data as well as with the theoretical energy-level

**Table X. PZC Parameters for the Corrosion Inhibition Effect of Green Tea Extract on MS in 1.0 M HCl**

Inhibitor	Concentration (g L <sup>-1</sup> )	E <sub>corr</sub> (mV)	PZC (mV)	E <sub>T</sub> (mV)
Blank 1 M HCl	0	-486	-569	83
GT 1	50	-479	-532	53
	100	-466	-509	43
	150	-460	-491	31
	200	-451	-474	23
GT 2	50	-481	-528	47
	100	-469	-507	38
	150	-454	-479	25
	200	-443	-461	18

calculations, which suggests that the adsorption of tea catechin monomers were mainly through the physical mode.

#### IV. CONCLUSIONS

The two commercial green tea extracts showed comparable inhibition properties for the corrosion of MS in 1 M HCl medium. The pct IE obtained via polarization measurement is in good agreement with that obtained by using the weight-loss and impedance methods. The polarization results also revealed that both inhibitors control the corrosion through the mixed mode of inhibition. Both the tea extracts were found to obey the Langmuir adsorption isotherm, and the thermodynamic parameters prove the physical adsorption of the phytoconstituents. This mode of adsorption is supported by PZC and molecular modeling studies. The HPLC technique proved to be an indispensable tool for the simultaneous determination of the active components of the green tea extracts that are responsible for the inhibition of MS corrosion. The adsorption capacity of catechin monomers increased in the following order: EC < EGC < ECG < EGCG. What is remarkable is that only catechins with the correct stereochemistry was involved in the inhibition process, whereas the mass of the other components (although present in high concentration as in the case for caffeine) remains unchanged. The findings underline the mandatory chemical analysis (both quantitative and qualitative) that is required when assessing the corrosion properties involving multicomponents (e.g., natural products). In contrast to previous studies, caffeine was shown conclusively not to be active in the anticorrosion process.

#### ACKNOWLEDGMENTS

The authors acknowledge gratefully the financial support of this work by the short-term Grant 304/PKIMIA/6310028 from the Universiti Sains Malaysia and university research Grant (1001/PKIMIA/832057).

#### REFERENCES

1. M. Sazuka, S. Murakami, M. Isemura, K. Satoh, and T. Nukiwa: *Cancer Lett.*, 1995, vol. 98, pp. 27–31.
2. T. Kakuda: *Biol. Pharm. Bull.*, 2002, vol. 25, pp. 1513–18.
3. M. Sano, M. Suzuki, T. Miyase, K. Yoshino, and M. Maeda-Yamamoto: *J. Agr. Food Chem.*, 1990, vol. 47, pp. 1906–10.
4. J. Hamilton-Miller: *Agents Chemother.*, 1995, vol. 39, pp. 2375–77.
5. V.W. Setiawan, Z.F. Zhang, G.P. Yu, Q.Y. Lu, Y.L. Li, M.L. Lu, M.R. Wang, C.H. Guo, S.Z. Yu, and R.C. Kurtz: *Int. J. Cancer*, 2001, vol. 92, pp. 600–04.
6. L. Zhong, M.S. Goldberg, Y.T. Gao, J.A. Hanley, M.É. Parent, and F. Jin: *Epidemiology*, 2001, vol. 12, pp. 695–700.
7. A. Crozier, I.B. Jaganath, and M.N. Clifford: *Nat. Prod. Rep.*, 2009, vol. 26, pp. 1001–43.
8. M.H. Hussin and M.J. Kassim, *Mater. Chem. Phys.*, 2011, vol. 125, pp. 461–468.
9. R.P. Bothi, R.A. Abdul, O. Hasnah, and A. Khalijah: *Acta Phys. Chim. Sin.*, 2010, vol. 26, pp. 2171–76.
10. M. Hosseini, M. Ehteshamzadeh, and T. Shahrabi: *Electrochim. Acta*, 2007, vol. 52, pp. 3680–85.
11. H. Tavakoli, T. Shahrabi, and M. Hosseini: *Mater. Chem. Phys.*, 2008, vol. 109, pp. 281–86.
12. R.A. Prabhu, T.V. Venkatesha, A.V. Shanbhag, G.M. Kulkarni, and R.G. Kalkhambkar: *Corros. Sci.*, 2008, vol. 50, pp. 3356–62.
13. P. Kern, D. Landolt, and Y. Abboud: *J. Electrochem. Soc.*, 2001, vol. 237, pp. B228–35.
14. A.J. Aldykewicz, H.S. Isaacs, and A.J. Davenport: *J. Electrochem. Soc.*, 1995, vol. 142, pp. 3342–50.
15. B. Müller: *React. Funct. Polym.*, 1999, vol. 39, pp. 165–77.
16. P.B. Raja and M.G. Sethuraman: *Mater. Lett.*, 2008, vol. 62, pp. 113–16.
17. P.B. Raja and M. Sethuraman: *Mater. Corros.*, 2009, vol. 60, pp. 22–28.
18. J. Buchweishaija and G. Mhinzi: *Portugaliae Electrochim. Acta*, 2008, vol. 26, pp. 257–65.
19. A.A. Rahim, E. Rocca, J. Steinmetz, and M. Jain Kassim: *Corros. Sci.*, 2008, vol. 50, pp. 1546–50.
20. A. Rahim and J. Kassim: *Recent Pat. Mater. Sci.*, 2008, vol. 1, pp. 223–31.
21. A.M. Shah, A.A. Rahim, S.A. Hamid, S. Yahya, and P.B. Raja: *Pigm. Resin Technol.*, 2010, vol. 40, pp. 118–22.
22. P.B. Raja and M. Sethuraman: *J. Mater. Eng. Perform.*, 2010, vol. 19, pp. 761–66.
23. P.B. Raja and M.G. Sethuraman: *Mater. Lett.*, 2008, vol. 62, pp. 2977–79.
24. A.Y. El-Etre, M. Abdallah, and Z. El-Tantawy: *Corros. Sci.*, 2005, vol. 47, pp. 385–95.
25. A.Y. El-Etre: *Corros. Sci.*, 2003, vol. 45, pp. 2485–95.
26. M.G. Sethuraman, P. Vadivel, and K.P.V. Kumar: *J. Electrochem. Soc. India*, 2001, vol. 50, pp. 143–46.
27. T. Fallavena, M. Antonow, and R.S. Gonçalves: *Appl. Surf. Sci.*, 2006, vol. 253, pp. 566–71.
28. S. Rajendran, A.J. Amalraj, M.J. Joice, N. Anthony, D.C. Trivedi, and M. Sundaravadivelu: *Corr. Rev.*, 2004, vol. 22, pp. 233–48.
29. A.A. Rahim, E. Rocca, J. Steinmetz, M.J. Kassim, R. Adnan, and M.S. Ibrahim: *Corros. Sci.*, 2007, vol. 49, pp. 402–17.
30. K.H. Row and Y. Jin: *Bioresour. Technol.*, 2006, vol. 97, pp. 790–93.
31. K.H. Khaled: *Int. J. Electrochem. Sci.*, 2008, vol. 3, pp. 462–75.
32. M.H. Hussin and M.J. Kassim: *J. Phys. Sci.*, 2010, vol. 21, pp. 1–14.
33. M. Benabdellah, R. Touzani, A. Aouniti, A. Dafali, S. El Kadiri, B. Hammouti, and M. Benkaddour: *Mater. Chem. Phys.*, 2007, vol. 105, pp. 373–79.
34. G.Y. Elewady: *Int. J. Electrochem. Sci.*, 2008, vol. 3, pp. 1149–61.
35. F. Bentiss, M. Lebrini, M. Lagrenée, M. Traisnel, A. Elfarouk, and H. Vezin: *Electrochim. Acta*, 2007, vol. 52, pp. 6865–72.
36. M. Morad and A. El-Dean: *Corros. Sci.*, 2006, vol. 48, pp. 3398–412.
37. M. Hosseini, S.F.L. Mertens, and M.R. Arshadi: *Corros. Sci.*, 2003, vol. 45, pp. 1473–89.
38. X. Li, S. Deng, and G. Mu: *Corros. Sci.*, 2009, vol. 51, pp. 620–34.
39. R. Solmaz, G. Kardaş, M. Çulha, B. Yazici, and M. Erbil: *Electrochim. Acta*, 2008, vol. 53, pp. 5941–52.

40. H. Wang, K. Helliwell, and X. You: *Food Chem.*, 2000, vol. 68, pp. 115–21.
41. P.L. Fernández, F. Pablos, M.J. Martín, and A.G. González: *J. Agric. Food Chem.*, 2002, vol. 50, pp. 1833–39.
42. E. Nishitani and Y.M. Sagesaka: *J. Food Compos. Anal.*, 2004, vol. 17, pp. 675–85.
43. F. de Souza and A. Spinelli: *Corros. Sci.*, 2009, vol. 51, pp. 642–49.
44. M.S. Maola, O.A. Arotiba, P.G.L. Baker, W.T. Mabusela, N. Jahed, E.A. Songa, and E.I. Iwuoha: *Int. J. Electrochem. Sci.*, 2009, vol. 4, pp. 1497–1510.
45. G. Blustein, R. Romagnoli, J. Jaén, A. Di Sarli, and B. del Amo: *Colloid Surf. Physicochem. Eng. Aspect*, 2006, vol. 290, pp. 7–18.
46. G. Gece: *Corros. Sci.*, 2008, vol. 50, pp. 2981–92.
47. Y. Yan, W. Li, L. Cai, and B. Hou: *Electrochim. Acta*, 2008, vol. 53, pp. 5953–60.
48. R. Solmaz, M. Mert, G. Kardas, B. Yazici, and M. Erbil: *Acta Phys. Chim. Sin.*, 2008, vol. 24, pp. 1185–91.
49. M. Lebrini, M. Lagrenée, H. Vezin, L. Gengembre, and F. Bentiss: *Corros. Sci.*, 2005, vol. 47, pp. 485–505.
50. M. Zhang, R. Ye, Y. Long, and Y. Chang: *J. Rare Earths*, 2011, vol. 29, pp. 138–42.
51. K. Mallaiya, R. Subramaniam, S.S. Srikandan, S. Gowri, N. Rajasekaran, and A. Selvaraj: *Electrochim. Acta*, 2011, vol. 55, pp. 3857–63.